

Influence of Yb-doping on optoelectrical properties of CdO nanocrystalline films

A. A. Dakhel

Received: 29 June 2010/Accepted: 21 September 2010/Published online: 1 October 2010
© Springer Science+Business Media, LLC 2010

Abstract Yb-doped CdO thin films with different Yb contents were prepared on glass and silicon substrates by vacuum evaporation technique. The effects of Yb-doping on the structural and optoelectrical properties of the host CdO films were systematically studied. The X-ray diffraction study shows that some of Yb^{3+} ions substituted for Cd^{2+} and the solubility of Yb in CdO is very limited and may be around ~ 0.2 at.%. The Yb-doping influences all the optoelectrical properties of CdO. The bandgap of Yb-doped CdO suffers narrowing by about 20% with a very small (0.03 at.%) doping level. The electrical behaviours show that all the prepared Yb-doped CdO films are degenerate semiconductors. Their dc-conductivity, carrier concentration, and mobility increase compared with undoped CdO film. The largest mobility of about $87 \text{ cm}^2/\text{V s}$ was measured for 0.13 at.% Yb-doped CdO film. From transparent-conducting-oxide point of view, Yb is sufficiently effective for CdO-doping.

Introduction

Cadmium oxide (CdO) thin films have a wide range of applications in optoelectronics [1, 2]. These applications are based on its unique properties. It can be an n-type semiconductor of relatively low electrical resistivity (10^{-2} – $10^{-4} \Omega \text{ cm}$) and transparent in visible and near infrared (VIS–NIR) spectral regions with a direct bandgap of 2.2–2.7 eV [1, 3–6]. CdO material crystallises in a cubic structure of $Fm\bar{3}m$ space group of 6-coordination with a cell

parameter of 0.4695 nm [7]. Its optoelectrical properties can be controlled through doping with different metallic ions like In, Sn, Al, Sc, Y, Tl, Ti, Al, etc., which improves its electrical conduction and increases its optical bandgap [1, 8–14]. Furthermore, it is possible to dope CdO with magnetic ions like Fe [15] to combine some magnetic properties with its normal optoelectronic properties for different applications. In addition, it is also possible to dope it with rare-earth 4f-ions like Sm or Dy [16, 17]. In this study, ytterbium was used as dopant to CdO to improve its conduction properties. This study reports the electrical and optical properties of Ytterbium-doped CdO films with different doping levels. As expected, when Yb ions of valence 3 substitute for some Cd^{2+} ions in CdO crystalline structure, the concentration of conduction electrons would be increased that improves the electrical conduction. Furthermore, it was observed that when the dopant ions have a smaller radius than that of Cd^{2+} ions then the conductivity of the doped CdO film would be increased, and the host CdO lattice unit cell compresses. In the present case the 6-coordination ionic radius of Cd^{2+} ion (0.0947 nm) is slightly more than that of Yb^{3+} ion (0.0868 nm) [18]. It must be mentioned that, the doping of CdO with Yb ions by any technique has not yet been reported.

Experimental details

CdO thin films doped with ytterbium of different levels were grown on glass and silicon substrates. The detailed deposition procedure has been described elsewhere [16]. The starting materials, Yb element and CdO (from Fluka A.G., Germany) were evaporated alternatively (layer-by-layer) with alumina baskets (Midwest tungsten service, USA). The substrates were ultrasonically clean glass and

A. A. Dakhel (✉)
Department of Physics, College of Science, University of Bahrain, PO Box 32038, Salmabad, Kingdom of Bahrain
e-mail: adakhil@sci.uob.bh

chemically (using HF) cleaned silicon wafer held in a vacuum chamber of residual oxygen atmosphere of pressure about 1.3×10^{-2} Pa. The as-grown films were totally oxidised and stabilised by annealing in air at 400°C for 2 h and then cooled slowly in a closed furnace. All the samples including the reference undoped CdO film were prepared in almost the same conditions.

The evaporated masses were controlled with a piezo-electric sensor using a Philips FTM 5 thickness monitor connected the sample holder. After annealing, the film thicknesses were measured using an MP100-M spectrometer (Mission Peak Optics Inc., USA) to be in the range 0.15–0.24 μm. The structure of the prepared films was studied by the X-ray diffraction (XRD) method using a Philips PW 1710 θ -2θ system with Cu K α radiation (0.15406 nm) and a step size of 0.02°. The energy-dispersive X-ray fluorescence (EDXRF) method was used to determine the relative weight fraction Yb to Cd in the studied samples. The setup used for the EDXRF method consists of an X-ray beam obtained from a Cu-anode Philips tube (Philips PW-1710) and an Amptek XR-100CR detector. The plan of this study is to prepare and study low Yb-doping level samples and one more sample of higher doping level to observe the possibility of formation of Yb-oxide grains inside the host medium CdO (i.e., nanocomposite film). The spectral optical transmittance $T(\lambda)$ and reflectance $R(\lambda)$ were measured at normal incidence in UV–VIS–NIR spectral region (300–3000 nm) with a Shimadzu UV-3600 double beam spectrophotometer. The electrical measurements were carried out with a standard Van-der-Pauw method with aluminium dot contacts in a magnetic field of about 1 T and using a Keithley 195A digital multimeter and a Keithley 225 current source.

Results and discussion

Characterisation by X-rays

Figure 1 demonstrates the energy-dispersive X-ray fluorescence (EDXRF) spectra for two prepared samples of Yb-doped CdO films on silicon substrate. The spectrum shows the Cd L-band (3.13–3.53 keV) and Yb L α -signal (7.41 keV) with signals from silicon substrate and exciting source. The ratio of integral intensity of Yb L α -signal (I_{Yb}) to that of Cd L-signal (I_{Cd}) or ($I_{\text{Yb}}/I_{\text{Cd}}$) was used to determine the relative weight fraction of Yb to Cd in a film sample. For that purpose, the known method of micro radiographic analysis (determination of mass ratio from X-ray intensity ratio) was used [19]. The reference samples were pure Yb₂O₃ and CdO thin films. The Yb content in film samples was varied. From the resulting Yb wt%, the at.% ratios were calculated to be 0.03, 0.13, 0.19, 0.21,

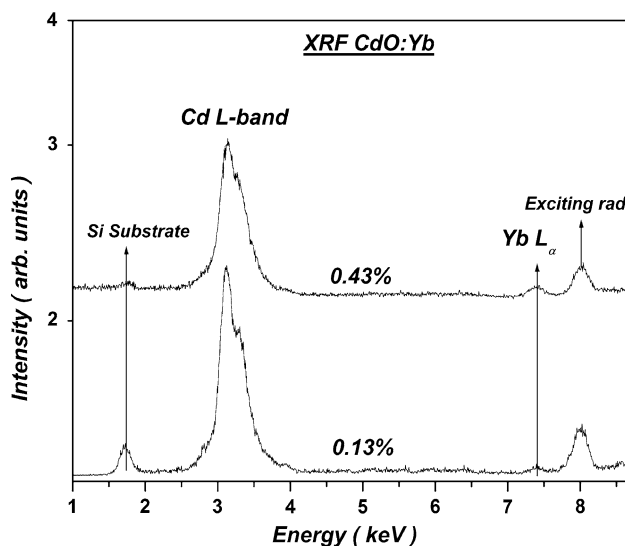


Fig. 1 X-ray fluorescence of Yb-doped CdO film grown on Si substrate. The exciting radiation was Cu K α

0.24, 0.43, and 1.8%. Each sample was named according its content of Yb at.%.

Figure 2 shows the X-ray diffraction (XRD) patterns of the prepared undoped and Yb-doped CdO films. The patterns reveal that all the investigated films are polycrystalline of cubic $Fm\bar{3}m$ CdO structure [7]. The possibility of formation of crystalline Yb oxide together with CdO was studied precisely by the XRD, as shown in Fig. 3. For low Yb doping level, almost all the Yb is incorporated into the CdO structure and no signal from Yb-oxide structure is detected. However, by increasing the at.% ratio to 1.8%, it was observed the presence of a weak reflection at about 29.7°, which was indexed to be the (222) reflection of

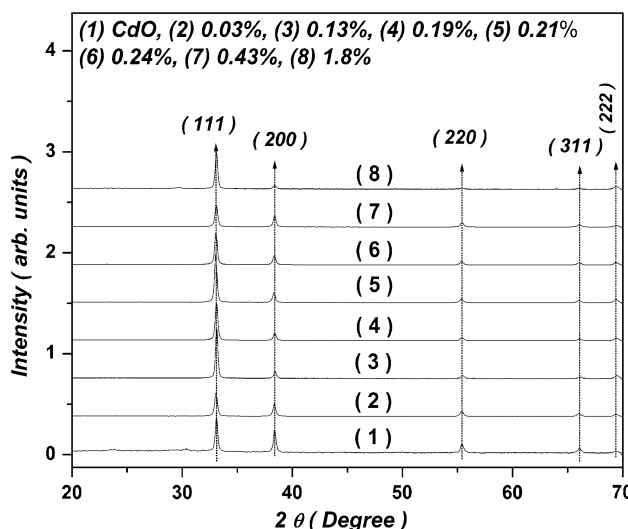


Fig. 2 X-ray diffraction patterns from undoped and Yb-doped CdO films. The used radiation was Cu K α -line

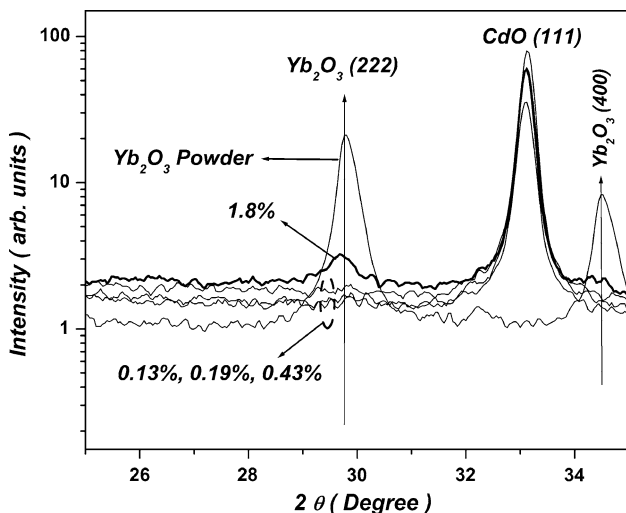


Fig. 3 X-ray diffraction from Yb_2O_3 and Yb-doped CdO films around (111) peak position of Yb_2O_3

crystalline Yb_2O_3 of BCC Ia3 (bixbyite) structure of $a = 1.0439 \text{ nm}$ [20]. The grain size of the found Yb_2O_3 nanograins was about 18 nm. Thus, one can deduce that the solubility of Yb in CdO is very limited and may be around ~ 0.2 at.% (see below).

The energetically favourable (111) preferred orientation growth of CdO films prepared by different techniques [21, 22], is studied here through the texture coefficient (TC). It is defined [23] as,

$$\text{TC}(hkl) = [nI_r(hkl)/I_{\text{std}}(hkl)] / [\sum_{k=1}^n I_r^k(hkl)/I_{\text{std}}^k(hkl)] \quad (1)$$

where $I_r(hkl)$ is the relative intensity of reflection from a given (hkl) plane, $I_{\text{std}}(hkl)$ is the relative intensity of the reflection from the same plane as indicated in a standard polycrystalline sample (ref.[7]), and n is the total number of reflections observed, which is four: (111), (200), (220), and (311). The calculated values of TC are given in Table 1 and inset of Fig. 4, which shows that the largest TC among low doping level films is 2.89 out of 4 for 0.13%. However, TC(111) is also increased to 3.25 out of 4 for the composite-oxides (Yb-doped CdO + Yb_2O_3) 1.8 at.% film.

The grain size (GS) perpendicular to [111] direction was determined using Scherrer equation [24] to be in the range 34–41 nm. The lattice parameter (a) and unit-cell volume (v_{cell}) are calculated by least squares method (LSM) and the results are given in Table 1 and Fig. 4. It is observed that, the unit-cell volume of host CdO film is smaller than that in the bulk pressed-powder disc. It is likely that the smaller unit cell arises because of the presence of vacancies inside the crystalline structure of the CdO film (nonstoichiometric composition) that cause the electrical conduction in the film. Doping with ytterbium slightly decreases

Table 1 The lattice parameter (a), average X-ray grain size (GS), and the texture coefficient [TC(111)] of the prepared undoped and Yb-doped CdO films of different % Yb fraction on glass substrates

Sample	a (nm)	GS (nm)	TC(111)
Powder	0.46948		
CdO	0.46806	34.7	1.38
0.03%	0.46829	34.7	1.6
0.13%	0.46732	41.7	2.89
0.19%	0.46743	34.7	2.58
0.21%	0.46874	34.7	2.55
0.24%	0.46853	34.7	2.37
0.43%	0.46782	34.7	1.72
1.80%	0.46783	41.7	3.25

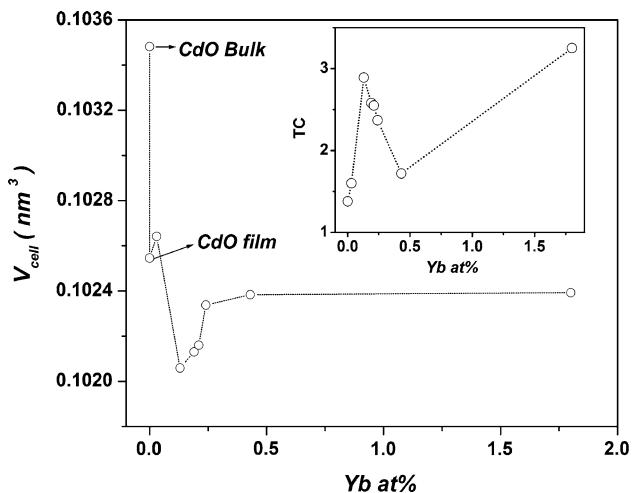


Fig. 4 Variation of host CdO unit-cell volume (v_{cell}) with the Yb at.% doping level. The inset shows the variation of TC with the Yb at.% doping level

v_{cell} to lowest value for 0.13 at.% film. However, for all the doped films the unit cell decreases with Yb-doping. This means that some of the Yb^{3+} ions of smaller size substituted for Cd^{2+} according to the following defect reaction in Kroger–Vink notation: $\text{Yb}_2\text{O}_3 \xrightarrow{\text{CdO}} \text{Yb}_{\text{Cd}}^{\bullet} + \text{O}_0^x + e'$ where $\text{Yb}_{\text{Cd}}^{\bullet}$ is the substitution of Yb^{3+} for Cd^{2+} in CdO lattice, O_0^x is the interstitial defect of oxygen atoms, and e' is an electron. Such doping creates structural strain that reduces v_{cell} , i.e., a slight decrease of lattice parameter of order $\sim 0.1\%$ was observed.

DC-electrical properties

The room temperature electrical resistivity (ρ), mobility (μ_{el}), and carrier concentration (N_{el}) were measured by a standard Van-der-Pauw method and the results are presented in Table 2 and Fig. 5. The main source of experimental error caused by aluminium-lead spots size was

Table 2 Summary of the measured electrical parameters

Sample	ρ ($\times 10^{-4} \Omega \text{ cm}$)	μ_{el} ($\text{cm}^2/\text{V s}$)	N_{el} (10^{20} cm^{-3})	E_g (eV)	$(N_{\text{el}}/\mu_{\text{el}})_{\text{elect}}$	$(N_{\text{el}}/\mu_{\text{el}})_{\text{opt}}$
CdO	201	7.03	0.44	2.42	0.63	0.321
0.03%	4.53	28.80	4.79	1.93	1.66	3.50
0.13%	1.37	87.22	5.22	2.29	0.60	2.35
0.19%	3.33	39.00	4.82	2.23	1.23	1.63
0.21%	4.86	36.86	3.48	2.24	0.94	2.67
0.24%	4.80	41.64	3.12	2.16	0.75	2.34
0.43%	6.53	27.82	3.43	2.00	1.23	3.42
1.80%	33.50	9.80	1.90	1.89	1.93	0.50

Resistivity (ρ), mobility (μ_{el}), and carrier concentration (N_{el}), and bandgap (E_g) of undoped and Yb-doped CdO films of different % Yb fraction. The ratio ($N_{\text{el}}/\mu_{\text{el}}$) measured optically (opt) and electrically (elect) are given in units ($\times 10^{29} \text{ V s/m}^3$)

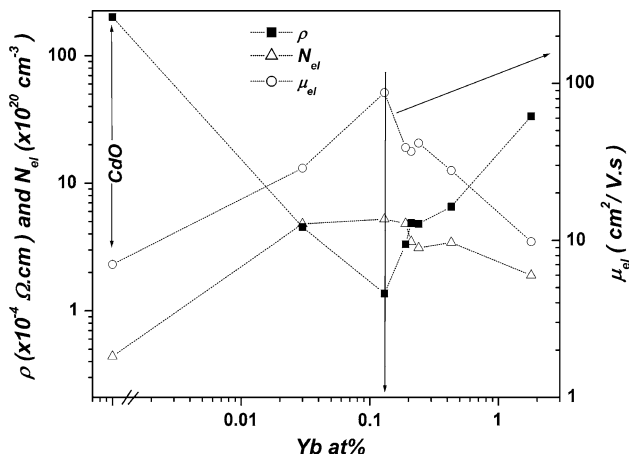


Fig. 5 Variation of resistivity (ρ), mobility (μ_{el}), and carrier concentration (N_{el}) for undoped and Yb-doped CdO films

estimated to be about 5%. The results show that undoped and all the Yb-doped CdO samples are n-type semiconductors. The measured electrical parameters (ρ , N_{el} , and μ_{el}) of undoped CdO film agree with those data published for CdO films prepared by different techniques but the resistivity is higher than those values mentioned in some other references $\sim 10^{-3}$ – $10^{-4} \Omega \text{ cm}$ due to different method and procedure of preparation [1]. For all the studied Yb-doped CdO films, the conductivity (σ), carrier concentration, and mobility increase in comparison with undoped CdO film. These changes result from the variation in N_{el} and carrier scattering by different microstructural defects, grain boundaries, and ionised impurities. Doping with Yb ions includes substitution of Yb^{3+} ions for Cd^{2+} ions (Yb_{Cd}), which liberates more conduction electrons in the conduction band. The N_{el} reaches the maximum value of $5.22 \times 10^{20} \text{ cm}^{-3}$ at Yb content of 0.13 at.%. This N_{el} remains almost unchanged until 0.19%, after which it decreases due to two reasons. The first reason is the grain boundary (GB) effect. The GB effect increases because the accumulation of Yb oxide reduces the conductivity by

reducing the carrier concentration and forming a potential barrier between the grains. The second reason is that both Yb_{Cd} and Yb_i are donors, and hence the increase of $\text{Yb}_{\text{Cd}}^{\bullet}$ and Yb_i^{\bullet} ions would result in enhancement of V_{Cd}'' acceptors to keep the charge balance in the system. This explanation is reasonable for the decrease in N_{el} when the Yb content is higher than 0.19 at.%. It must be emphasised that the obtained high mobility, especially the value $87.22 \text{ cm}^2/\text{V s}$ for Yb content of 0.13 at.%, arises despite the obviously simple preparation technique. The increase of the mobility can be attributed to the improvement of crystallinity. Thus, the sample that has maximum mobility also has maximum texture coefficient and larger grain size (Table 1). The decrease of the mobility for doping level more than 0.13 at.% is attributed to the scattering by ionised impurity and GBs enhanced by Yb oxide accumulation. Generally, Yb dopant with low concentration plays principally the same role as other usual non rare-earth metallic dopants.

In summary, the results of this study show that low doping with Yb improves the dc-conduction parameters of CdO films, so that the 0.13 at.% Yb-doped CdO film shows an increase in its mobility by about 12.4 times, conductivity by 147 times, and carrier concentration by 12 times compared with undoped film. Almost identical variations were also observed in CdO films doped with Sm, Dy, and Eu [16, 17, 25]. The overall variations of the conduction parameters in this case result from the complication of the process of Yb incorporation in CdO films. For Yb concentration up to 0.13 at.%, the main mechanism that controls the incorporation is the substitution of Yb^{3+} ions for Cd^{2+} ions and occupying interstitial locations. However, for dopant levels more than 0.13 at.%, the Yb accumulation at GBs starts gradually to be the predominant mechanism. For high doping level, 1.8 at.%, Yb begins to form isolated Yb_2O_3 nanograins. The grain size of Yb_2O_3 grains, as determined from peak broadening using Scherrer equation, is about 18 nm. Thus, one can deduce that the solubility of Yb in CdO is very limited and may be around

~0.2 at.%, which supports the conclusion of the structural study. In addition, with the above-described discussion one can explain the variation in the effective concentration of the carriers that participate in the dc-conduction process.

Optoelectronic properties

The spectral optical absorption method is used to study the optical properties of the prepared Yb-doped CdO films grown on corning glass substrates. The experimentally corrected normal spectral transmittance $T(\lambda)$ and reflectance $R(\lambda)$ in the UV–VIS–NIR region (300–3000 nm) are presented in Fig. 6. The spectra show that the maxima of the spectral transmittance for all the investigated films are in the NIR region. In addition, in NIR region, the transmittance curves show a clear damping due to high density of the free electrons. The normal reflectance for all the samples studied in UV, VIS, and NIR is almost constant and close to each other in magnitude of 1–5%. The spectral absorption coefficient $\alpha(\lambda)$ is calculated from the experimental data using the following equation [26]: $\alpha(\lambda) = (1/d) \ln[(1 - R)/T]$, where d is the film thickness. The optical direct bandgap E_g is evaluated according to the well-known energy-exponential relation [27]:

$$\alpha E = A_{\text{Op}}(E - E_g)^m \quad (2)$$

where A_{Op} is a constant and the exponent m is equal to 0.5 or 2 for direct and indirect transitions, respectively. Thus, the plot of $(\alpha E)^2$ versus E as shown in Fig. 7 gives the value of direct bandgap. The obtained bandgaps for undoped and Yb-doped CdO films are given in Table 2 and Fig. 8 (plotted in semi log scale to show all the experimental points). For undoped CdO, the bandgap is obtained in the range of (2.2–2.6 eV) that is known for undoped CdO films prepared by different techniques [1]. As

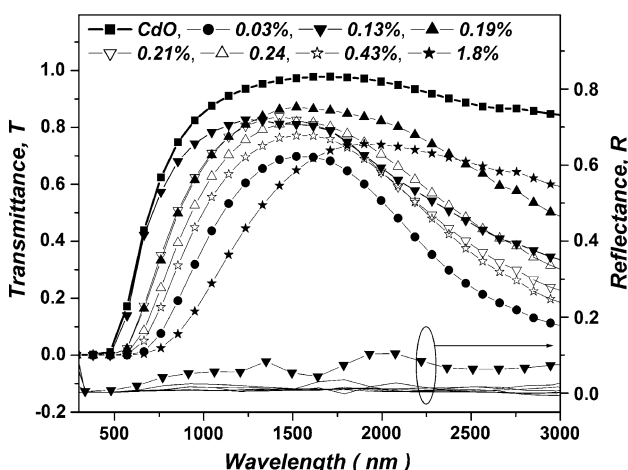


Fig. 6 Spectral normal transmittance and reflectance in the UV–VIS–NIR spectral regions for undoped and Yb-doped CdO films

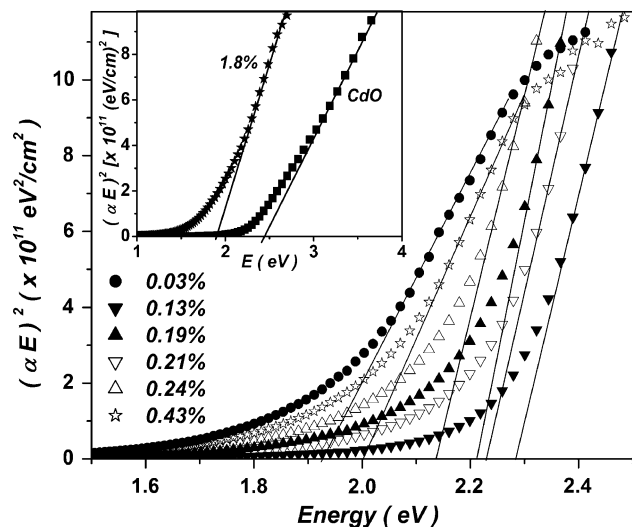


Fig. 7 Calculated (points) spectral optical absorption coefficient α is plotted as $(\alpha E)^2$ versus photon energy (E) for Yb-doped CdO films. The inset shows the bandgap determination plot for CdO and 1.8% films

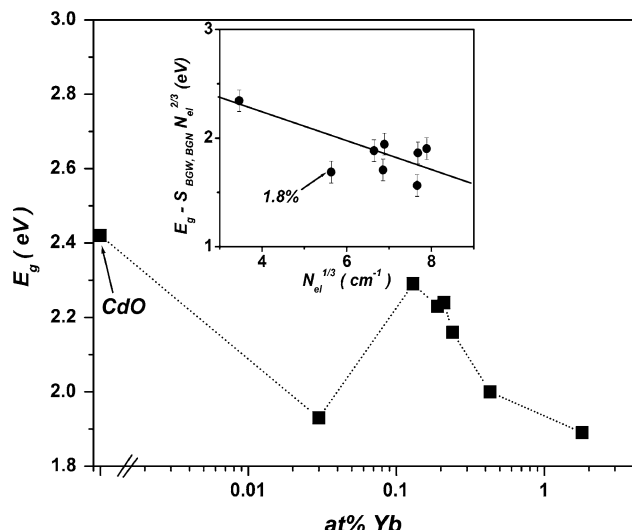


Fig. 8 Dependence of the bandgap (E_g) on the dopant at.% levels of Yb-doped CdO films. The inset shows the dependence of optoelectronic function ($E_g - S_{\text{BGW},\text{BGN}} N_{\text{el}}^{2/3}$) on $N_{\text{el}}^{1/3}$. The straight line represents the best fit

mentioned in “Introduction” section, doping of CdO with different metals can widen the CdO bandgap [28, 29]. It is observed that the bandgaps of all the Yb-doped CdO films are narrower than that of undoped CdO film. The bandgap was suddenly decreased by 20% for the 0.03% sample. Such bandgap narrowing (BGN) is observed to be associated with an increase in the carrier concentration by about 11 times and, thus, it contrasts the bandgap widening (BGW) or Moss–Burstein (B-M) effect [30, 31]. This BGN comes as consequence of a change in the nature and

strength of the crystalline potential by addition the influence of Yb^{3+} impurity dopant ions including the effect of their 4f-electrons on the crystalline electronic states. Thus, due to the doping, the band tailing or impurity band becomes broader, finally reaches, and merges the bottom of the conduction band causing decrease in the effective optical bandgap E_g . Phenomenologically, it is possible to relate the bandgap variations with the carrier concentration. The BGW (or ΔE_g^{BM}) for parabolic band approximation is given by the following relation [32]:

$$\Delta E_g^{\text{BM}} = \text{BGW} = S_{\text{BGW}} N_{\text{el}}^{2/3} \quad (3)$$

where $S_{\text{BGW}} = (\hbar^2 / 2\gamma m_e)(3\pi^2)^{2/3}$, \hbar is the Plank's constant and $\gamma = m_{\text{vc}}^*/m_e$ is the ratio for of reduced effective mass to free-electron mass, which is equal to 0.274 for CdO [33]; thus $S_{\text{BGW}}^{\text{th}} = 1.348 \times 10^{-18} \text{ eV m}^2$.

The BGN consists of two parts. The first part arises due to the electron-impurity interaction and is given by the following relation [34, 35] $\Delta E_{\text{bt}} = S_{\text{BGN}}^{(1)} N_{\text{el}}^{2/3}$, where $S_{\text{BGN}}^{(1)} = (1/3)S_{\text{BGW}} = 4.49 \times 10^{-19} \text{ eV m}^2$. The second part of BGN results from Columbic interaction (C-int) between the carriers and is given by [36, 37] $\Delta E_{\text{C-int}} = S_{\text{BGN}}^{(2)} N_{\text{el}}^{1/3}$, where $S_{\text{BGN}}^{(2)} = (e/2\pi\epsilon_0\epsilon_r)(3/\pi)^{1/3}$, ϵ_0 is the permittivity of free space, e is the electronic charge, and for the dielectric constant ϵ_r it is possible to use ϵ_∞ , thus $S_{\text{BGN}}^{(2)} = 2.836 \times 10^{-9}/\epsilon_r$. Therefore, the total BGN is:

$$\text{BGN} = (S_{\text{BGN}}^{(1)} N_{\text{el}}^{2/3} + S_{\text{BGN}}^{(2)} N_{\text{el}}^{1/3}) \quad (4)$$

The overall bandgap shift is:

$$\begin{aligned} \Delta E_g &= E_g - E_{g0} = \text{BGW} - \text{BGN} \\ &= S_{\text{BGW}} N_{\text{el}}^{2/3} - S_{\text{BGN}}^{(1)} N_{\text{el}}^{2/3} - S_{\text{BGN}}^{(2)} N_{\text{el}}^{1/3} + C_f \\ &= S_{\text{BGW,BGN}} N_{\text{el}}^{2/3} - S_{\text{BGN}}^{(2)} N_{\text{el}}^{1/3} + C_f \end{aligned} \quad (5)$$

where C_f is the fitting parameter and $S_{\text{BGW,BGN}} = S_{\text{BGW}} - S_{\text{BGN}}^{(1)} = 8.98 \times 10^{-19} \text{ eV m}^2$. In this study, a good straight line was obtained by considering the plot of $[E_g - S_{\text{BGW,BGN}} N_{\text{el}}^{2/3}]$ vs. $N_{\text{el}}^{1/3}$, as shown in the inset of Fig. 8, with $S_{\text{BGN}}^{(2)} = 1.31 \times 10^{-9} \text{ eV m}$. This value is close to the theoretical one [1, 36] $S_{\text{BGN}}^{(2)}(\text{th}) = 1.107 \times 10^{-9} \text{ eV m}$. As long as the theoretical basis for the above models is the parabolic band approximation, then it is possible to explain the slight difference might come from the non-parabolic band effects, especially we are doping with magnetic 4f-metal.

In the NIR spectral region, where the reflectivity is almost constant, the absorption coefficient α is related to the wavelength according to [25, 38] $\alpha(\lambda) = B_{\text{Op}}\lambda^2$ where $B_{\text{Op}} = 5.243 \times 10^{-13}(N_{\text{el}}/\mu_{\text{el}})_{\text{Opt}}(1/n\gamma^2)$ in unit system SI, where n is the refractive index at NIR region ($n = 1.6$). Thus by neglecting of the small variations of n in the NIR, a linear

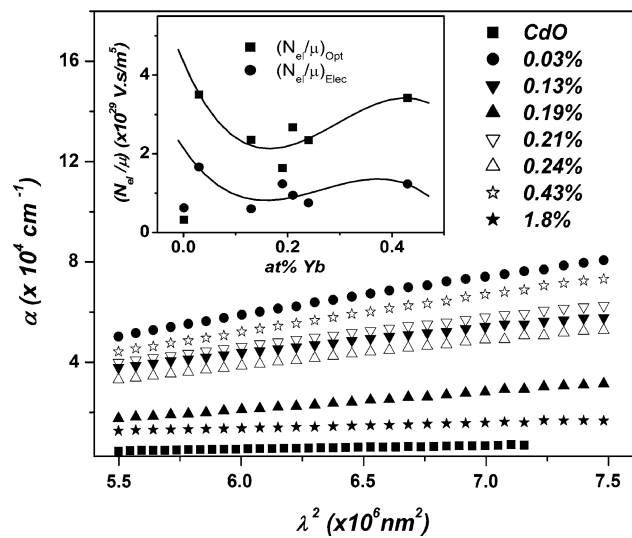


Fig. 9 The dependence of absorption coefficient α on λ^2 in the NIR spectral region for undoped and Ce-doped CdO films. The inset shows the dependence of the (N_{el}/μ) ratio measured optically and electrically, on the Yb % doping level of Yb-doped CdO films

α vs. λ^2 relationship should be observed, as shown in Fig. 9. Thus, it is possible to estimate the ratio $(N_{\text{el}}/\mu_{\text{el}})_{\text{opt}}$ and the results are given in Table 2. The value of $(N_{\text{el}}/\mu_{\text{el}})_{\text{elec}}$ (measured electrically) should be different from $(N_{\text{el}}/\mu_{\text{el}})_{\text{opt}}$ (measured optically) due to different conduction mechanisms. However, the inset of Fig. 9 shows similar trends of the variation for both $(N_{\text{el}}/\mu_{\text{el}})_{\text{elec}}$ and $(N_{\text{el}}/\mu_{\text{el}})_{\text{Opt}}$ up to 0.43 at.% Yb, after which a clear predominant effect of the Yb accumulation on GBs that makes the optical and electrical measured ratios very different from each other (Table 2).

Conclusions

The structural and optoelectrical properties of Yb-doped CdO films were investigated in the present work. The XRD study shows that some of Yb^{3+} ions of smaller size substituted for Cd^{2+} and the solubility of Yb in CdO film is very limited and may be around ~ 0.2 at.%. Optical investigations show that the low doping with Yb ions (0.03 at.%) causes abrupt reduction the bandgap of the host CdO by about 20%. For all the studied Yb-doping levels, the dc-conductivity, carrier concentration, and mobility increase compared with undoped CdO films, so that the 0.13 at.% Yb-doped CdO film shows an increase in its mobility by about 12.4 times, conductivity by 147 times, and carrier concentration by 12 times compare with undoped film. The largest mobility of about $87 \text{ cm}^2/\text{V s}$ was observed for 0.13% Yb-doped CdO film. From

transparent-conducting-oxide point of view, Yb is a very effective dopant for CdO doping.

References

- Zhao Z, Morel DL, Ferekides CS (2002) *Thin Solid Films* 413:203
- Gurumurugan K, Mangalaraj D, Narayandass SAK (1996) *J electron Mater* 25:765
- Carballeda-Galicia DM, Castanedo-Perez R, Jimenez-Sandoval O, Jimenez-Sandoval S, Torres-Delgado G, Zuniga-Romero CI (2000) *Thin Solid Films* 371:105
- Chopra KL, Ranjan S (1993) *Thin film solar cells*. Plenum Press, New York
- Choi YS, Lee CG, Cho SM (1996) *Thin Solid Films* 289:0153
- Kondo R, Okimura H, Sakai Y (1971) *Jpn J Appl Phys* 10:1547
- Powder Diffraction File, Joint Committee for Powder Diffraction Studies (JCPDS), File no. 05-0640
- Maity R, Chattopadhyay KK (2006) *Solar Energy Mater Solar Cells* 90:597
- Shu S, Yang Y, Medvedova JE, Ireland JR, Metz AW, Ni J, Kannewurf CR, Freeman AJ, Tobin TJ (2004) *J Am Chem Soc* 126:13787
- Gupta RK, Ghosh K, Patel R, Mishra SR, Kahol K (2008) *Mater Lett* 62:3373
- Wang A, Babcock JR, Edleman NL, Metz AW, Lane MA, Asahi R, Dravid VP, Kannewurf CR, Freeman AJ, Marks TJ (2001) *Appl Phys Sci* 98:7113
- Dakhel AA (2008) *Phys Status Solidi (a)* 205:2704
- Gupta RK, Ghosh K, Patel R, Kahol PK (2009) *Appl Surf Sci* 255:6252
- Gupta RK, Ghosh K, Patel R, Mishra SR, Kahol PK (2009) *Curr Appl Phys* 9:673
- Dakhel AA (2010) *Thin Solid Films* 518:1712
- Dakhel AA (2009) *J Alloys Compd* 475:51
- Dakhel AA (2009) *Sol Energy* 83:934
- Shannon RD (1976) *Acta Crystallogr A* A32:751
- Jaklevic JM, Goulding FS (1978) In: Herglotz HK, Birks LS (eds) *X-ray spectrometry*. Marcel Dekker Inc, New York, p 50
- Gschneidner KA, Eyring LeRoy (eds) (1982) *Handbook on the physics and chemistry of rare Earths*, vol 15. Holland publication company, Amsterdam, p 575
- Subramanyam TK, Uthanna S, Naidu BS (1998) *Mater Lett* 35:214
- Reddy KTR, Sravani C, Miles RW (1998) *J Cryst Growth* 184(185):1031
- Barrett CS, Massalski TB (1980) *Structure of metals*. Pergamon, Oxford, p 204
- Kaelble EF (ed) (1967) *Handbook of X-rays for diffraction, emission, absorption, and microscopy*. McGraw-Hill, New York, pp 17–50
- Dakhel AA (2009) *Opt Mater* 31:691
- Hong WQ (1989) *J Phys D Appl Phys* 22:1384
- Tauc J, Abeles F (ed) (1969) *Optical properties of solids*. North Holland
- Gupta RK, Ghosh K, Patel R, Kahol PK (2009) *Appl Surf Sci* 255:4466
- Saha B, Thapa R, Chattopadhyay KK (2008) *Solid State Commun* 145:33
- Mergel D, Qiao Z (2002) *J Phys D Appl Phys* 35:794
- Dua LK, De A, Chakraborty S, Biswas PK (2008) *Mater. Charact* 59:578
- Burstein E (1954) *Phys Rev* 93:632
- Kawamura K, Maekawa K, Yanagi H, Hirano M, Hosono H (2003) *Thin Solid Films* 445:182
- Hahn D, Jaschinski O, Wehmann HH, Schlachetzki A (1995) *J Electron Mater* 24:1357
- Bugajski M, Lewandowski W (1985) *J Appl Phys* 57:521
- Wolff PA (1962) *Phys Rev* 126:405
- Camassel J, Auvergne D, Mathieu H (1975) *J Appl Phys* 46:2683
- Hartnagel HL, Dawar AL, Jain AK, Jagadish G (1995) *Semi-conducting transparent thin films*. IOP, Bristol